JOURNAL OF AIRCRAFT
Vol. 35, No. 3, May–June 1998

Aerodynamic Optimization Using Sensitivity Derivatives from a Three-Dimensional Supersonic Euler Code

Vamshi Mohan Korivi*
Old Dominion University, Norfolk, Virginia 23529-0247
Perry A. Newman†
NASA Langley Research Center, Hampton, Virginia 23681-2199
and
Arthur C. Taylor III‡
Old Dominion University, Norfolk, Virginia 23529-0247

Initial results from a three-dimensional marching Euler code equipped with an efficient sensitivity analysis capability are presented. The aerodynamic sensitivity derivatives with respect to wing geometry parameters obtained by the incremental iterative method are compared with those obtained by an efficient central finite differencing method and are both accurate and computationally cheaper. Sample cases for a Mach 2.4 high-speed civil transport wing–body configuration are shown that indicate the feasibility of using these sensitivity derivatives in aerodynamic optimization studies. These demonstrations have been given for design variables that determine wing planform and control flap deflections. The filleted wing–body geometry and computational fluid dynamics grid are modified by automated surface geometry and grid generation codes through which sensitivity information is propagated.

Introduction

THE use of current advanced computational fluid dynamics (CFD) analysis codes in design optimization studies and applications via sensitivity analysis (SA) requires the efficient and accurate calculation of sensitivity derivatives (SD). The incremental iterative method (IIM) was proposed and demonstrated to provide such SD from a two-dimensional thin-layer Navier–Stokes code for both nongeometric (flow) and geometric (shape) design variables in Refs. 1 and 2. In addition to accurate, consistent discrete SD obtained with computational efficiency (in terms of both CPU time and memory requirements), the IIM also allows the use of approximate solution operators of choice for greater efficiency, parallelization, or robustness, etc. Initial results from a three-dimensional marching Euler code for SD with respect to nongeometric design variables have appeared in Ref. 3. The present paper demonstrates an efficient calculation of geometric (shape) SD with respect to wing planform and control-flap deflection design variables (DV) for a three-dimensional marching Euler code. Sensitivity derivatives for these DV as well as those with respect to wing-section thickness and camber parameters have been generated for a filleted wing–body configuration that approximates a Mach 2.4 high-speed civil transport (HSCT) and were reported in Ref. 4. The wing planform and control-flap deflection SD are highlighted because of their close relationship to structural shape design and stability and control studies, respectively.

Presented as Paper 94-4270 at the AIAA/USAF/NASA/ISSMO 5th Symposium on Multidisciplinary Analysis and Optimization, Panama City Beach, FL, Sept. 7–9, 1994; received Oct. 26, 1996; revision received Nov. 13, 1997; accepted for publication Nov. 13, 1997.

*Graduate Research Assistant, Mechanical Engineering Department; currently Project Engineer, Optimal CAE, Inc., Novi, MI 48375-5377.

†Senior Research Scientist, Multidisciplinary Optimization Branch, Fluid Mechanics and Acoustics Division, M/S 159.

‡Associate Professor, Mechanical Engineering Department, KDH 238. Member AIAA.

The three-dimensional Euler equations are solved for a fully supersonic flow with the space-marching method described in Ref. 5. The method is an upwind cell-centered finite volume scheme that is higher-order-accurate (second-order in the streamwise direction and third-order in the cross plane) and fully conservative in all directions, including the streamwise (marching) direction. The method is locally time iterative in each cross plane with a spatially split, approximate factorization approach.

Because the grid-generation and flow-analysis codes are separate entities, the coupling of these two disciplines to obtain aerodynamic (flow) SD with respect to geometric (grid) design variables involves the transfer of not only the grid but also the grid sensitivities. The aerodynamic optimization studies subsequently performed also involve these two disciplines, which are coupled sequentially, i.e., no feedback, at each optimization step. Sample cases for a Mach 2.4 HSCT configuration are shown that demonstrate the feasibility of using these SD in aerodynamic or multidisciplinary studies.

Two other works also present results for the aerodynamic optimization of three-dimensional wings with Euler equations and analytical derivatives or adjoint (costate) variables. Both were for transonic flows with a subsonic freestream; therefore, the studies have employed elliptic-like grids and more complex mixed-flow-solver algorithms. Burgreen and Baysal[6] and Burgreen[7] considered both wing section and planform design variables and implemented discrete SA with an optimizer. Jameson[8] considered wing-section variables for a fixed planform and implemented an optimization technique based on control theory. The present approach is conceptually similar to that of Refs. 6 and 7; however, most of the details differ with respect to the surface parameterization, the grid generation and differentiation, the CFD flow solver, the linear SD solver, and the optimizer. The present paper will not address these details at a level sufficient to point out the differences; the primary purpose here is a twofold demonstration of efficiency and accuracy of aerodynamic SD obtained via IIM and the feasibility of using SD via IIM in optimization studies.

Aerodynamic Sensitivity Derivatives

An overview of recent research activities that have concentrated on the efficient and accurate calculation of SD from

advanced CFD codes is given in Ref. 9. The IIM is among the most accurate and efficient method yet proposed or demonstrated; the results presented herein are the initial three-dimensional geometric SD obtained from this method. Because the method has been outlined in Refs. 3 and 9, the theory and equations will not be repeated here. The recent work of Burgreen and Baysal[6] and Burgreen[7] also makes use of the IIM with a preconditioned conjugate gradient type of solver to obtain SD from the three-dimensional Euler equations for a transonic wing. In the present work as well as that presented in Refs. 6–8, the required differentiation of the flow codes has been by hand. Initial two-dimensional results from automatic differentiation of a flow code to obtain SD via IIM are given in Ref. 10.

Nongeometric Variables

Figure 1 is a view of the HSCT 24E configuration generated at NASA Langley Research Center, including the wake portion of the computational grid (37 streamwise $\times$ 121 circumferential $\times$ 15 normal) used in the nongeometric variable study of Ref. 3. Grid refinement studies to determine the adequacy of the computed solutions for modeling the detailed physical aspects of the flow have not been carried out. This study addresses the consistency of solution SD computed by two different means and their initial use in sample aerodynamic optimization problems. The consistency aspect of the SD is independent of the number of points in the computational grid; however, well-converged solutions on the chosen grid are required to verify this consistency.

Comparisons of SD results for the six-component force and moment coefficients (C_x, C_y, C_z, C_{M_x}, C_{M_y}, C_{M_z}) with respect to nongeometric (flow) variables have been given in the expanded version of Ref. 3 and will not be repeated here. These SD were computed by both forward finite differences and the quasianalytical IIM; the calculated SD ratios (forward finite differences, at a perturbation step of 1.E−05, to quasianalytical derivatives) were unity to four significant figures. However, the computational cost of the SD obtained by a finite difference method was greater than that for the IIM.

Geometric Variables

Most modern advanced CFD analysis codes use body-fitted computational grids that are required as input. That is, the grid generation for a specified configuration is not part of the flow code but rather a separate entity. This separation has several consequences in regard to flow sensitivity analysis with respect to geometric or shape design variables. First, these variables are only implicitly seen by the CFD code through their effect on the generated body-fitted grid i.e., these variables set the boundary conditions in the grid-generation code. Second, the CFD grid generation appears to be a separate discipline. This separate discipline now must be coupled to the flow code not only through the body-fitted grid but also through its SD with respect to either the geometric variables that specify the configuration or those that are deemed to be design variables. Several approaches can be taken to obtain these latter SD of the grid (or grid movement) with respect to design variables; these approaches and related matters are also discussed in Ref. 9.

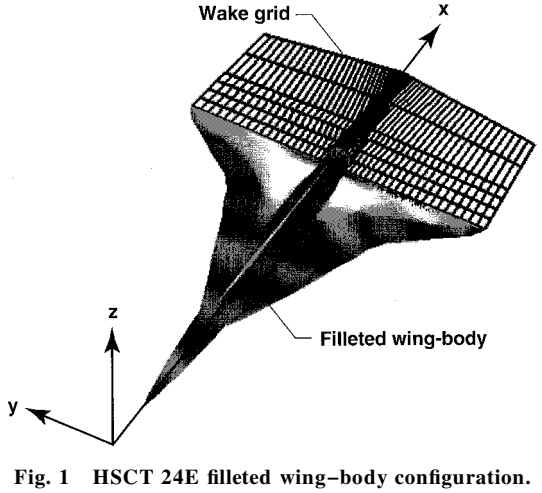

Fig. 1 HSCT 24E filleted wing–body configuration.

Automated Geometry and Grid Generation

The geometry processing and grid-generation codes used here[11,12] take as their input simplified numerical descriptions of configuration parts in a wave-drag, or Harris, format. The various component surfaces are first intersected and filleted[11] into a continuous surface; then suitable computational grids are generated.[12] For the present study, geometric SD are propagated from a design variable parameterization of the HSCT 24E configuration through these surface processing and volume grid-generation codes. These latter codes have been linked together, front-ended with a 42-variable wing geometry parameterization,[13] and automatically differentiated. Unger's parameterization[13] of the HSCT 24E wing geometry is divided into three variable types: 1) seven planform variables, 2) 15 section-thickness variables (five each at the root, break, and tip sections), and 3) 20 camber surface variables. The geometry parameterization used herein is discussed in Ref. 4 and in the appendix; the camber parameterization used by Unger has been replaced and flap descriptions added. As in Ref. 13, propagation of the geometric SD through the automated geometry package is accomplished with the automatic differentiation (AD)[14,15] precompiler tool ADIFOR (automated differentiation of Fortran).[16–18] Execution of the ADIFOR-enhanced automated geometry package then calculates not only the grid but also the grid SD with respect to the design variables that are used in the geometry parameterization. Both are required as input to the flow code that has been differentiated by hand.

Comparison of Sample SD Results

A number of sample results that compare the SD obtained by central finite differences and the IIM are given for several geometric variables of each type in Ref. 4. These results are computed on a half-space grid (only 49 points in the circumferential direction with a symmetry plane at $y = 0$) so that some forces, moments, and SD are not balanced by their images and, therefore, do not vanish. These nonvanishing components do not affect the geometric SD comparisons for the six-component force and moment coefficient (C_x, C_y, C_z, C_{M_x}, C_{M_y}, C_{M_z}) SD with respect to geometric design variables. In obtaining SD via central finite difference approximations (SD_{FD}) analysis solutions at design variable perturbations ($\sim 10^5$) from the baseline were run from restart solution files and converged to a relative residual reduction of 10^{-11}. This process results in an appreciable time savings in obtaining SD_{FD}, at least for the present CFD algorithm and code. In obtaining SD via IIM (SD_{QA}), the relative derivative-residual reduction was done to several levels: 10^{-3} [three orders of magnitude (OM)], 10^{-7} (7 OM), and 10^{-11} (11 OM). Comparisons are given in Ref. 4 for both accuracy and computational efficiency.

Six SDs with respect to the four outboard flap deflections are compared in Table 1. This table has three parts: Table 1a gives the 24 SD_{QA} values; Table 1b shows the 24 ratios SD_{FD}/SD_{QA} for 11 OM convergence; and Table 1c gives computational timing results. Table 1a shows that these derivatives range in size over 4 orders of magnitude and are both positive and negative. Table 1b shows that the SD_{QA} agree with the SD_{FD} to between three and four significant figures. Table 1c shows the computation of SD_{QA} to be more than 2.5 times faster than that obtained from the efficient SD_{FD}, i.e., with restarts, central finite difference time is about 0.88 rather than 8 times a baseline analysis solution time. The speedup depends

Table 1 Comparison of geometric flap deflection sensitivity derivatives for HSCT 24E at $M_\infty = 2.4$, $\alpha = 1$ deg, $\beta = 0$ deg

	Scaled design variables, D			
SD_{QA}	Flap I	Flap II	Flap III	Flap IV
a: Quasianalytical sensitivity derivatives of force and moment coefficients				
$\frac{\partial C_x}{\partial D}$	+7.7336E−06	+5.5417E−06	+7.2944E−08	+7.3339E−07
$\frac{\partial C_y}{\partial D}$	−6.5184E−06	+2.3167E−05	−4.4830E−08	+5.5264E−06
$\frac{\partial C_z}{\partial D}$	−2.1190E−04	+9.6692E−04	−4.6974E−06	+2.8558E−04
$\frac{\partial C_{M_x}}{\partial D}$	−3.0110E−05	+1.2727E−04	−9.2512E−07	+5.5924E−05
$\frac{\partial C_{M_y}}{\partial D}$	+5.8343E−05	−3.1718E−04	+1.5573E−06	−9.7259E−05
$\frac{\partial C_{M_z}}{\partial D}$	−3.6965E−06	+9.5445E−06	−3.0774E−08	+2.0969E−06
$\frac{SD_{FD}}{SD_{QA}}$	Design variables, D			
	Flap I	Flap II	Flap III	Flap IV
b: Sensitivity derivative ratios, $\frac{\text{finite difference}}{\text{quasianalytical}}$, except terms of $\mathcal{O}(\varepsilon)$				
$\frac{\partial C_x}{\partial D}$	0.9999	0.9999	[a]	[a]
$\frac{\partial C_y}{\partial D}$	1.0002	1.0001	[a]	0.9997
$\frac{\partial C_z}{\partial D}$	0.9999	1.0000	0.9998	1.0003
$\frac{\partial C_{M_x}}{\partial D}$	0.9999	1.0000	0.9998	1.0006
$\frac{\partial C_{M_y}}{\partial D}$	0.9999	1.0000	0.9998	1.0006
$\frac{\partial C_{M_z}}{\partial D}$	1.0000	1.0000	[a]	1.0003
Solution method		Number of solutions		Ratio
c: Computational timing comparisons				
Baseline		1		1.000[b]
Central finite difference		8		0.877
Quasianalytical		4		0.3439

[a]Ratio for extremely small quantities is meaningless.
[b]Baseline solution run time for $(R^n_{\text{rms}}/R^1_{\text{rms}})$ reduction to $\varepsilon \equiv 10^{-11}$ on Cray-2 is 152 s.

on the SD accuracy required and the analysis code convergence performance from restarts.

Similar comparisons of the six SD with respect to three wing planform variables are shown in Table 2. Here, SD comparisons are shown at the 7-OM convergence level. Several SD with respect to root chord (RC) appear to have much larger discrepancies between the SD_{FD} and the corresponding SD_{QA} than expected; that is, much better agreement (to several significant figures) has been shown for SD with respect to all other geometric variables.[4] The discrepancies appear to be about 5% for $\partial C_z/\partial$RC and about 1% for both $\partial C_{M_y}/\partial$RC and $\partial C_{M_x}/\partial$RC. The SD_{FD} with respect to RC were sensitive to the perturbation step size; at perturbation step sizes of both 10^{-4} and 10^{-7} the comparisons were worse than those shown. With this exception, the SD_{QA} agree with the SD_{FD} to about four significant figures; in addition, they are obtained faster with the IIM.

Aerodynamic Optimization

The purpose of these initial studies is simply to indicate the feasibility of using the SD obtained by the IIM in aerodynamic or multidisciplinary optimization. Additional applications of the three-dimensional marching Euler code with efficient geometric SD calculations for aerodynamic optimization studies are given in Ref. 4. The automated design synthesis (ADS) program[19] is used for the optimization code in these studies, in a black box fashion. In Ref. 4, the design variables for thickness, camber, flap deflection, and planform were activated separately to ascertain whether the predicted changes were reasonable when only a supersonic cruise point had been considered. The fact that other discipline codes are not participating requires that side constraints be specified on the design variables, i.e., with no structural input, minimum thickness must be set. Use of the ADS code requires that three options must be selected; a strategy, an optimizer, and a one-dimensional search.[19] For the present constrained optimization results, the sequential quadratic programming strategy, the modified method of feasible directions optimizer, and the Golden section line search options have been selected. Both function and first-order derivative (SD) information is given to the ADS code. Because the SD via IIM are local derivatives, this combination of methods in ADS appears to give the most consistent opti-

Table 2 Comparison of geometric planform sensitivity derivatives for HSCT 24E at $M_\infty = 2.4$, $\alpha = 1$ deg, $\beta = 0$ deg

SD_{FD} / SD_{QA}	Scaled design variables, D		
	Root chord	Break chord	Tip chord
a: Quasianalytical sensitivity derivatives of force and moment coefficients			
$\frac{\partial C_x}{\partial D}$	−1.5421E−02	+1.0243E−03	+2.1698E−05
$\frac{\partial C_y}{\partial D}$	+1.6117E−01	−5.0936E−04	+7.1228E−05
$\frac{\partial C_z}{\partial D}$	+4.7495E−03	+7.7265E−04	+4.6021E−05
$\frac{\partial C_{M_x}}{\partial D}$	+7.1231E−04	+1.1721E−04	+1.7400E−05
$\frac{\partial C_{M_y}}{\partial D}$	−7.9255E−03	−1.9745E−04	−2.3264E−05
$\frac{\partial C_{M_z}}{\partial D}$	+2.4522E−02	−2.9745E−04	−5.9707E−05
SD_{FD} / SD_{QA}	Design Variables, D		
	Root chord	Break chord	Tip chord
b: Sensitivity derivative ratios, $\frac{\text{finite difference}}{\text{quasianalytical}}$ (7 OM reduction)			
$\frac{\partial C_x}{\partial D}$	0.9993	0.9999	0.9999
$\frac{\partial C_y}{\partial D}$	1.0005	0.9999	1.0000
$\frac{\partial C_z}{\partial D}$	1.0490	1.0000	1.0000
$\frac{\partial C_{m_x}}{\partial D}$	1.0058	1.0000	0.9999
$\frac{\partial C_{M_y}}{\partial D}$	1.0102	1.0001	1.0000
$\frac{\partial C_{M_z}}{\partial D}$	1.0011	0.9999	0.9999

Solution method	Number of solutions	Ratio
c: Computational timing comparisons		
Baseline	1	1.000[a]
Central finite difference	6	1.322
Quasianalytical (3 OM)	3	0.2046
Quasianalytical (7 OM)	3	0.2829
Quasianalytical (11 OM)	3	0.3606

[a]Baseline solution run time for $(R^n_{\text{rms}}/R^1_{\text{rms}})$ reduction to $\varepsilon \equiv 10^{-11}$ on Cray-2 is 152 s.

mization results. However, many function evaluations are required by the selected search procedure.

HSCT Studies

The HSCT 24E filleted wing–body configuration generated by NASA Langley Research Center is the baseline for these shape design improvement studies. The HSCT 24*E* configuration resulted from multidisciplinary preliminary design procedures that included a camber surface optimization based on linear aerodynamics. Structural optimization studies have also been performed[20] on this configuration. In Ref. 4, sample studies for shape optimization are done separately for 15 wing thickness variables, 28 and 8 wing camber variables, as well as those for the four flap-deflection variables and five wing planform design variables shown herein. For these studies, the flow conditions are Mach number $M_\infty = 2.4$, angle of attack $\alpha = 1$ deg, and yaw angle $\beta = 0$ deg. Convergence of both the nonlinear iterative flow analysis and the linear iterative SA was required to a relative residual reduction of 6 OM for all required solutions. Extensive use was made of restart solution files for the flow analysis solutions.

Lift Improvement

For these lift improvement studies, the objective function is lift maximization while the wing-root bending moment and drag are constrained to their baseline values; that is,

$$\text{minimize } -C_z/C_{Z_0}$$

$$\text{subject to } C_{M_x}/C_{M_{x_0}} \leq 1.0, \quad C_x/C_{X_0} \leq 1.0$$

Side constraints on both the flap and planform design variables were also employed, but not violated in the sample studies given next.

Flap Deflection Variables

In multidisciplinary applications, all CFD solutions should be provided for at least an approximately deflected and trimmed configuration. As a first step into this multiple discipline interaction, the static balance and trim control surface deflections should be investigated for advanced CFD code solutions. Four outboard flaps were defined as part of the baseline HSCT 24E wing. Typically, the flaps would be designed at low speed, with takeoff and landing flow conditions. At high-speed flow conditions, these flaps might be deflected for trim and control purposes. An indication of their effectiveness for lift-improvement on the HSCT 24E is demonstrated by the sample results shown in Table 3. The objective and constraint functions were given in the preceding text. Table 3a shows that a 1% lift increase is obtained in five optimization steps (which required 76 function evaluations and five gradient evaluations). Both constraints are active (within ±0.5% of the baseline value). Initial and final values of the scaled flap deflections are shown in Table 3b.

In regard to the run time of the codes on the Cray-2, for a relative residual reduction of 6 OM with four design variables, the initial 99 s consists of about 67 s for an analysis run from a dead start and 32 s for the four SD evaluations by IIM. If all function evaluations, including those for central SD_{FD} required for this study, could be done from a dead start, i.e., uniform freestream, to the same 6-OM convergence level, then the total CPU time would have been about 7770 s or 2.16 Cray-2 h. The total run-time savings with the use of restart files is about 5600 s; the savings as a result of the use of SD via IIM is an additional 590 s. Note, however, that 1) the run-time savings as a result of using restart files is code dependent and appears to be large for the present analysis code; and 2) the run-time savings for using SD via IIM instead of SD_{FD} from a dead start would be about 2520 s.

Table 3 shows that the flap deflection SD for these outboard flaps are rather small compared with the SD for other geometric design variables, such as some of those in Table 2. Therefore, we did not try to trim the pitching moment for the HSCT 24E. Two studies were done, however, on a delta wing where larger inboard and outboard flaps were defined. In the first study, a lift improvement of 1.2%, with bending moment and drag constrained, was obtained in five optimization steps. In the second study, the pitching moment was changed about 8.6% in six optimization steps, with bending moment, lift, and drag constrained. Summary tables for these two studies are not included here.

Wing Planform Variables

Planform optimization should be multidisciplinary because input from other disciplines is required. Therefore, it is typically done 1) early in the design cycle at the conceptual or early preliminary design stage where these other disciplines participate, and 2) with linear aerodynamic codes. Generally, several (or more) discrete planforms are selected and section

Table 3 Wing flap deflection optimization study, four design variables, for HSCT 24E at $M_\infty = 2.4$, $\alpha = 1$ deg, $\beta = 0$

	Initial	Final	% Change
a: Design improvement summary			
Objective (C_z)	1.9087E−02	1.9309E−02	+1.01E+00
Constraint I (C_M)	8.4736E−04	8.4727E−04	−0.10E−02[b]
Constraint II (C_x)	1.9361E−03	1.9309E−03	+0.63E−05[b]
Number of function evaluations	1	76	——
Number of gradient evaluations	1	5	——
CPU (s)[a]	99	1581	——
Flap number	Initial value		Final value
b: Scaled flap deflection design variable changes			
I	0.0		−2.4125
II	0.0		+0.2644
III	0.0		+10.000
IV	0.0		−1.7263

[a]Run time on Cray-2 for 6 OM reduction in all analysis and sensitivity derivative residuals.
[b]Active constraint.

Table 4 Wing planform optimization study, five design variables, for HSCT 24E at $M_\infty = 2.4$, $\alpha = 1$ deg, $\beta = 0$ deg

	Initial	Final	% Change
a: Design improvement summary			
Objective (C_z)	1.9086E−02	2.0133E−02	+5.5
Constraint I (C_M)	8.4736E−03	8.4153E−04	−6.88
Constraint II (C_x)	1.9361E−03	2.0104E−03	+3.83[b]
Number of function evaluations	1	102	——
Number of gradient evaluations	1	4	——
CPU (s)[a]	132	2701	——
Design variable	Initial value	Final value	% Change
b: Scaled design variable changes			
Root chord	1.420	1.456	+2.52
Break chord	4.236	4.269	+3.24
Tip chord	9.303	1.488	−84.00
X break leading edge	9.965	10.358	+3.94
X tip leading edge	13.840	15.263	+10.28

[a]Run time on Cray-2 for 6 OM reduction in all analysis and sensitivity derivative residuals.
[b]Constraint violated.

variables are then optimized for each planform study. In the sample case presented in this section, lift optimization for constrained wing root bending moment and drag has been done with five planform variables (see Appendix); all other design variables are held at their baseline HSCT 24E values.

Results for lift optimization with respect to five planform variables are given in Table 4. A minimum (perhaps local) has been found in four optimization steps with a lift improvement of 5.5% and the drag constraint violated by 3.8%. Neither wing–root bending-moment constraint nor any of the design-variable side constraints are active or violated.

The baseline and optimized planforms are shown in Fig. 2. For supersonic flow considerations alone, the wing tip should be swept more than in the baseline HSCT 24E; Fig. 2 shows that the optimization procedure agrees with this result. At a Mach number of 2.4, the Mach angle is 24.6 deg. The angle subtended by the wing–tip leading edge from the root leading edge is 25.9 deg for the baseline HSCT 24E and 23.8 deg for the final optimized planform. That is, the planform optimized for only supersonic flow lies behind the Mach cone.

Planform optimizations with other objectives, such as drag minimization or lift/drag ratio maximization, and different design variables have been done; however, comprehensive conclusions were not drawn. In particular, for the optimization results just presented, the planform area changed. We have not constrained it, nor have we differentiated the geometry and grid-generation codes with respect to planform area to constrain it formally in the optimization. For the double trapezoidal wing planform this can be done with the three wing chords and two wingspans held fixed, which leaves only the inboard and outboard wing panel sweeps to change.

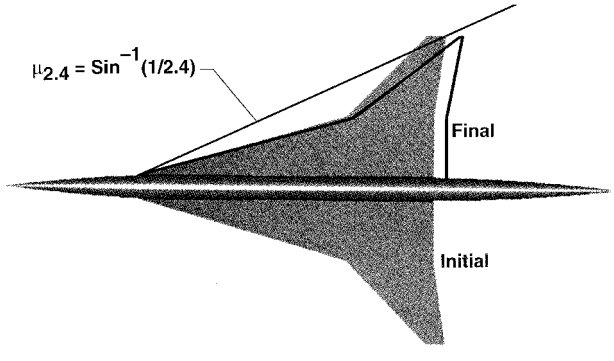

Fig. 2 Comparison of HSCT planforms for lift-improvement study.

Concluding Remarks

A computationally efficient general methodology has been successfully demonstrated for iteratively solving the large systems of linear equations required for obtaining quasianalytical sensitivity derivatives from three-dimensional CFD codes. Results have been shown for the coupling of automatic-differentiated geometry and grid-generation codes with a hand-dif-

ferentiated flow code to obtain geometric (shape) sensitivity derivatives and use them in sample aerodynamic optimization studies. Demonstrations have been given for design variables that determine wing planform and flap deflections.

Appendix: Wing Geometry Parameterization

The baseline HSCT 24E geometry generated at NASA Langley Research Center resulted from a multidisciplinary preliminary design based on linear aerodynamic codes; it is given in the wave-drag format. The wing is described at 18 span stations, which are located as shown in Table A1. The seven planform variables required to describe a double trapezoidal wing used in Ref. 13 and herein are root chord (RC), break chord (BC), tip chord (TC), x location of LE at break (XBC), x location of LE at tip (XTC), inboard span (IS), and outboard span (OS), and are also defined in Fig. A1. The inboard- and outboard-span variables are shown with dashed arrows because they were not involved in any of the present optimization studies.

Parameterization of wing-section thickness and camber for the HSCT 24E geometry is given in Ref. 4. The camber has been described at each wing station so that both leading- and trailing-edge flaps can be included. Locations of the four outboard flaps on the HSCT 24E are shown in Fig. A2. These locations are fixed in the present work and the flap deflections constitute the four control flap design variables. Additional spanwise control (or smoothing) is required to model the flap edge gaps and for the optimization design variable changes discussed in the text.

Table A1 HSCT 24E wing section locations

Wing section	% distance along span from side of fuselage
1 (Root)	0.00
2	5.94
3	11.88
4	17.82
5	23.77
6	29.71
7	35.65
8 (Break)	42.44
9	47.53
10	53.47
11	59.42
12	65.36
13	71.30
14	77.24
15	83.18
16	89.12
17	95.06
18 (Tip)	100.00

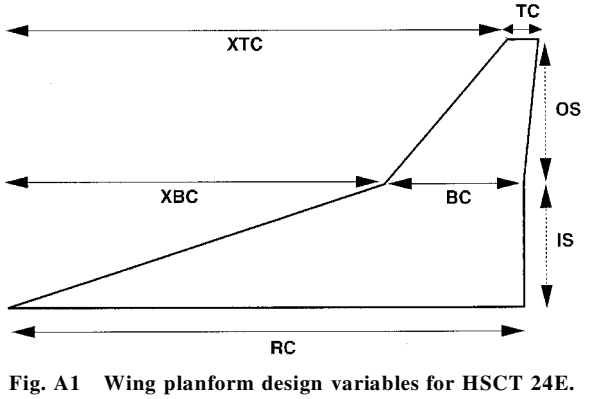

Fig. A1 Wing planform design variables for HSCT 24E.

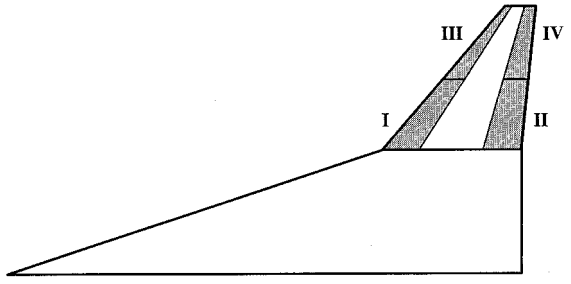

Fig. A2 Wing outboard flap locations for HSCT 24E.

Acknowledgments

This research was partially supported by Grant NAG-1-1265 from NASA Langley Research Center. We are indebted to Eric Unger for providing us the use of his HSCT 24E design variable parameterization and the linked differentiated geometry/grid-generation code package, to Gene Hou for discussions regarding optimization, to Ray Barger and Mary Adams for assistance with the geometry and grid generation codes, and to Peter Coen and Jim Fenbert for discussions in regard to the HSCT 24E configuration.

References

[1]Korivi, V. M., Taylor, A. C., III, Newman, P. A., Hou, G. J.-W., and Jones, H. E., "An Approximately-Factored Incremental Strategy for Calculating Consistent Discrete Aerodynamic Sensitivity Derivatives," *Journal of Computational Physics*, Vol. 113, No. 2, 1994, pp. 336–346; also AIAA Paper 92-4746, Sept. 1992.

[2]Newman, P. A., Hou, G. J.-W., Jones, H. E., Taylor, A. C. III, and Korivi, V. M., "Observations on Computational Methodologies for Use in Large-Scale Gradient-Based Multidisciplinary Design," *AIAA/USAF/NASA/OAI 4th Symposium on Multidisciplinary Analysis and Optimization*, Pt. 1, AIAA, Washington, DC, 1992, pp. 531–542.

[3]Korivi, V. M., Taylor, A. C., III, Hou, G. J.-W., Newman, P. A., and Jones, H. E., "Sensitivity Derivatives for Three-Dimensional Supersonic Euler Code Using Incremental Iterative Strategy," *AIAA 11th Computational Fluid Dynamics Conference*, Pt. 2, AIAA, Washington, DC, 1993, pp. 1053, 1054; also *AIAA Journal*, Vol. 32, No. 6, 1994, pp. 1319–1321.

[4]Korivi, V. M., Newman, P. A., and Taylor, A. C., III, "Aerodynamic Optimization Studies Using a 3-D Supersonic Euler Code with Efficient Calculation of Sensitivity Derivatives," *AIAA/USAF/NASA/ISSMO 5th Symposium on Multidisciplinary Analysis and Optimization*, Pt. 1, AIAA, Washington, DC, 1994, pp. 170–194.

[5]Newsome, R. W., Walters, R. W., and Thomas, J. L., "An Efficient Strategy for Upwind Relaxation Solutions to the Thin-Layer Navier-Stokes Equations," *AIAA Journal*, Vol. 27, No. 9, 1989, pp. 1165–1166; also AIAA Paper 87-1113, June 1987.

[6]Burgreen, G. W., and Baysal, O., "Three-Dimensional Aerodynamic Shape Optimization of Wings Using Sensitivity Analysis," AIAA Paper 94-0094, Jan. 1994.

[7]Burgreen, W. G., "Three-Dimensional Aerodynamic Shape Optimization of Wings Using Discrete Sensitivity Analysis," Ph.D. Dissertation, Old Dominion Univ., Norfolk, VA, May 1994.

[8]Jameson, A., "Optimum Aerodynamic Design Via Boundary Control," *Optimum Design Methods in Aerodynamics*, AGARD, FDP-VKI, Von Kàrmàn Inst., Rhode-St. Genese, Belgium, April 1994.

[9]Taylor, A. C., III, Newman, P. A., Hou, G. J.-W., and Jones, H. E., "Recent Advances in Steady Compressible Aerodynamic Sensitivity Analysis," *Flow Control, Mathematics and Its Applications*, edited by M. D. Gunsberger, Vol. 68, Springer–Verlag, New York, 1995, pp. 341–356.

[10]Sherman, L. L., Taylor, A. C., III, Green, L. L., Newman, P. A., Hou, G. J.-W., and Korivi, V. M., "First- and Second-Order Aerodynamic Sensitivity Derivatives Via Automatic Differentiation with Incremental Iterative Methods," *Journal of Computational Physics*, Vol. 129, 1996, pp. 307–336; also AIAA Paper 94-4262, Sept. 1994.

[11]Barger, R. L., and Adams, M. S., "Automatic Computation of Wing-Fuselage Intersection Lines and Fillet Inserts with Fixed-Area Constraint," NASA TM 4406, March 1993.

[12]Barger, R. L., Adams, M. S., and Krishnan, R. R., "Automatic Computation of Euler Marching Grids and Subsonic Grids for Wing-Fuselage Configurations," NASA TM 4573, July 1994.

[13]Unger, E. R., and Hall, L. E., "The Use of Automatic Differentiation in an Aircraft Design Problem," *AIAA/USAF/NASA/ISSMO 5th Symposium on Multidisciplinary Analysis and Optimization*, Pt. 1, AIAA, Washington, DC, 1994, pp. 64–72.

[14]Rall, L. B., "Automatic Differentiation: Techniques and Applications," *Recent Development and Applications*, *Lecture Notes in Computer Science and Mathematical Programming*, Vol. 120, Springer–Verlag, Berlin, 1981.

[15]Griewank, A., and Corliss, G. F. (eds.), *Automatic Differentiation of Algorithms: Theory, Implementation, and Application*, Society of Industrial and Applied Mathematics, Philadelphia, PA, 1991.

[16]Bischof, C. H., Carle, A., Corliss, G. F., Griewank, A., and Hovland, P., "ADIFOR: Generating Derivative Codes from Fortran Programs," *Scientific Programming*, Vol. 1, No. 1, 1992, pp. 1–29.

[17]Bischof, C. H., and Griewank, A., "ADIFOR: A Fortran System for Portable Automatic Differentiation," *AIAA/USAF/NASA/OAI 4th Symposium on Multidisciplinary Analysis and Optimization*, Pt. 1, AIAA, Washington, DC, 1992, pp. 433–441.

[18]Bischof, C. H, Carle, A., Corliss, G. F., Griewank, A., and Hovland, P., "Getting Started with ADIFOR. ADIFOR Working Note #9," Mathematics and Computer Science Division, Argonne National Lab., MCS-ANL-TM-164, Argonne, IL, 1992.

[19]Vanderplaats, G. N., "ADS—A Fortran Program for Automated Design Synthesis," NASA CR-17785, Sept. 1985.

[20]Barthelemy, J.-F. M., Wrenn, G. A., Dovi, A. R., Coen, P. G., and Hall, L. E., "Supersonic Transport Wing Minimum Weight Design Integrating Aerodynamics and Structures," *Journal of Aircraft*, Vol. 31, No. 2, 1994, pp. 330–338.